

# Extinction estimation over land ice using long-wavelength Pol-InSAR

Jayanti J. Sharma, Irena Hajnsek, Konstantinos P. Papathanassiou

Microwaves and Radar Institute, German Aerospace Center, Münchner Straße 20, 82234 Weßling, Germany

Email: jayanti.sharma@dlr.de, irena.hajnsek@dlr.de, kostas.papathanassiou@dlr.de

## Abstract

In recent years there has been increased interest in using SAR to study and monitor glaciers and ice sheets for glaciological and climate change research. This paper describes for the first time the estimation of ice extinction through the modelling of Pol-InSAR coherences as a combination of a surface contribution from the snow-ice interface and a volume response. Separation of the ground and volume contributions is obtained through decomposition of the polarimetric coherency matrix. Both model-based Freeman 2- and 3-component and eigenvector decompositions are examined. Ground-to-volume scattering ratios derived from polarimetry are used in conjunction with Pol-InSAR interferometric coherences to invert the extinction of the ice layer. Validation is performed with airborne Pol-InSAR data at L- and P-band collected using DLR's E-SAR system over the Austfonna ice cap in Svalbard, Norway as part of the ICESAR campaign.

## 1 Introduction

SAR is a powerful remote sensing tool with which to measure glaciers and ice sheets due to its high spatial resolution and wide coverage, and its ability to penetrate beneath the ice surface to observe sub-surface structures. However, SAR backscattering from ice remains poorly understood including the relative importance of scattering from surface and volume layers, and dependencies on frequency and glacier facie.

The objective of this paper is to isolate the volume response to enable estimation of the extinction of the ice volume at L- and P-band for the first time. In previous work, e.g. [1, 2], removal of the surface component was not considered in extinction estimation. Extinction is a relevant parameter for glaciologists since it contains information on the density and internal structure of the ice. Decoupling of the surface and volume responses is achieved using eigenvector and model-based polarimetric decompositions in section 2. Ground-to-volume scattering ratios from the polarimetric decomposition are then used in conjunction with Pol-InSAR coherences to estimate the extinction of the ice volume for experimental data. Results and discussion are presented in section 4, followed by a summary and a look to future work.

## 2 Modelling land ice extinctions

### 2.1 Volume isolation through PolSAR decomposition

To estimate the extinction of the ice volume, it is necessary to separate the ground and volume contributions. Here we estimate the ground-to-volume scattering ratios through decomposition of the polarimetric coherency matrix. Eigenvector decompositions [3] separating dominant scattering mechanisms as well as the model-based Freeman 3-component [4] and Freeman 2-component [5] decompositions yield estimates of the ground-to-volume scattering ratio at each polarisation. Each of these decompositions is briefly outlined below.

The eigenvalue problem can be used to generate a diagonal form of the coherency matrix  $[T]$ , yielding a general decomposition into independent scattering processes [3]:

$$[T] = [T_1] + [T_2] + [T_3] = [U_3][\Lambda][U_3]^{-1}, \quad (1)$$

where  $[\Lambda]$  is the diagonal eigenvalue matrix with elements  $(\lambda_1 \geq \lambda_2 \geq \lambda_3 \geq 0)$  and  $[U_3] = [e_1, e_2, e_3]^T$  is the unitary eigenvector matrix with columns corresponding to the orthonormal eigenvectors. We assume that the dominant scattering mechanism yielding coherency matrix  $[T_1] = \lambda_1(e_1 e_1^\dagger)$  is due to surface scattering. This assumption can be verified by examining the polarimetric properties of  $[T_1]$ . Eigenvector decomposition has the advantage in that no underlying model is assumed.

The Freeman 3-component decomposition (abbreviated Freeman-3) assumes that the signal consists of three components: surface and dihedral returns from reflection-symmetric media, and a volume component from a cloud of randomly oriented dipoles. Combined, this gives the following reflection-symmetric coherency matrix :

$$[T] = [T_s] + [T_d] + [T_v] \quad (2)$$
$$= f_s \begin{bmatrix} 1 & \beta^* & 0 \\ \beta & |\beta|^2 & 0 \\ 0 & 0 & 0 \end{bmatrix} + f_d \begin{bmatrix} |\alpha|^2 & \alpha & 0 \\ \alpha^* & 1 & 0 \\ 0 & 0 & 0 \end{bmatrix} + f_v \begin{bmatrix} 2 & 0 & 0 \\ 0 & 1 & 0 \\ 0 & 0 & 1 \end{bmatrix},$$

where  $s$  is surface,  $d$  is dihedral and  $v$  is volume, and  $f_s$ ,  $f_d$ ,  $f_v$ ,  $\alpha$  and  $\beta$  are parameters inverted from the model used to reconstruct  $[T_s]$ ,  $[T_d]$  and  $[T_v]$ .

In applying the Freeman 2-component model we assume that the surface response dominates, such that the returns are from a reflection-symmetric surface and a volume of particles characterised by a shape parameter  $\rho$ . Combined, this gives:

$$[T] = [T_s] + [T_v] \quad (3)$$
$$= f_s \begin{bmatrix} 1 & \beta^* & 0 \\ \beta & |\beta|^2 & 0 \\ 0 & 0 & 0 \end{bmatrix} + f_v \begin{bmatrix} 1 & 0 & 0 \\ 0 & \rho & 0 \\ 0 & 0 & \rho \end{bmatrix}.$$

Converting the coherency matrices into covariance matrices ( $[T] \rightarrow [C]$ ) provides a separation of the power contributions from the surface and from other components for each linear polarisation. Ground-to-volume scattering ratios  $\mathbf{m} = [m_{HH}, m_{HV}, m_{VV}]$  are then computed using the power along the diagonals of the covariance matrices:

$$\text{Eigenvector: } \mathbf{m} = \frac{\text{diag}([C_1])}{\text{diag}([C_2]) + \text{diag}([C_3])} \quad (4)$$

$$\text{Freeman-3: } \mathbf{m} = \frac{\text{diag}([C_s])}{\text{diag}([C_d]) + \text{diag}([C_v])} \quad (5)$$

$$\text{Freeman-2: } \mathbf{m} = \frac{\text{diag}([C_s])}{\text{diag}([C_v])}. \quad (6)$$

Note that both Freeman-3 and Freeman-2 models assume the surface power contributed by the cross-pol to be zero and thus  $m_{HV} = 0$ .

## 2.2 Extinction estimation using Pol-InSAR

The ground-to-volume scattering ratios estimated in the previous step are used in combination with Pol-InSAR interferometric coherences and a uniform-volume-plus-ground model for determination of the ice extinction coefficient.

The extinction  $\kappa_e$  accounts for the combined effect of absorption and scattering in the medium and may be expressed in terms of the penetration depth  $d_{\text{pen}}$  at which the one-way backscattered power falls to  $1/e$  given by [6]:

$$\kappa_e = -\cos \theta_r / d_{\text{pen}}, \quad (7)$$

where  $\theta_r$  is the refracted incidence angle in the ice volume and the  $\cos \theta_r$  factor accounts for the off-vertical travel distance of the wave within the medium.  $\kappa_e$  is the extinction coefficient in units of  $\text{m}^{-1}$ , although it is conventionally quoted in Nepers as  $\simeq 8.686 \cdot \kappa_e$  dB/m.

Let  $\gamma_z$  represent the coherence from a combination of volume scattering with complex coherence  $\gamma_{\text{vol}}$  and a surface scattering component at the snow-ice interface whose strength is determined by the positive scalar  $m$ . After correction of SNR and range spectral decorrelation the coherence magnitude is given as [7]:

$$|\gamma_z| = \left| \frac{\gamma_{\text{vol}}(\kappa_e) + m}{1 + m} \right|, \quad (8)$$

where, assuming an infinite, uniform volume  $\gamma_{\text{vol}}$  can be represented by:

$$\gamma_{\text{vol}} = \frac{1}{1 + \frac{j \cos \theta_r k_{z\text{vol}}}{2\kappa_e}}. \quad (9)$$

In Eq. 9  $j$  is the imaginary number and  $k_{z\text{vol}} = \frac{4\pi\sqrt{\epsilon}}{\lambda} \frac{\Delta\theta_r}{\sin \theta_r}$  is the vertical wave number in the volume;  $\lambda$  is the wavelength in free space,  $\epsilon$  the ice permittivity and  $\Delta\theta_r$  the difference in look angles from each antenna in the volume.

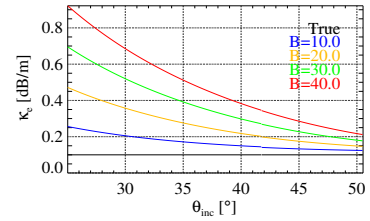
With knowledge of  $m$  from the polarimetric decompositions of section 2.1, we can solve for  $\kappa_e$  using Eqs. 8 and 9 at each polarisation and each pixel independently.

### 2.2.1 Simulations

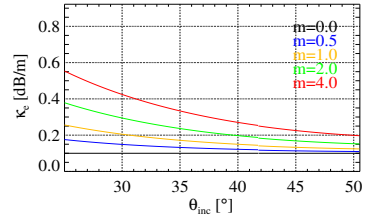
Given a measure of unbiased volumetric coherence  $\gamma_{\text{vol}}$ , the magnitude of Eq. 9 may be used to estimate the extinction  $\kappa_e$ :

$$\kappa_e = \frac{1}{\sqrt{\frac{1}{|\gamma_{\text{vol}}|^2} - 1}} \cdot \frac{\cos \theta_r k_{z\text{vol}}}{2}. \quad (10)$$

However, in the presence of a non-zero contribution from the snow-ice interface, i.e.  $m \neq 0$ , extinctions inverted using Eq. 10 will be biased. If the ice is homogeneous, extinction should have no incidence angle ( $\theta_{\text{inc}}$ ) dependency. If the surface scattering component is not taken into account during inversion, there are clear trends with incidence angle as seen in simulations in **Figure 1**, with the bias becoming greater for larger ground-to-volume scattering ratios  $m$  and longer baselines (translating to larger  $k_{z\text{vol}}$ ).



(a)  $\kappa_e$  for changing baseline,  $m = 1.0$



(b)  $\kappa_e$  for changing  $m$ ,  $B = 10\text{m}$

**Figure 1:** Simulated inverted P-band (0.35 GHz) extinctions assuming a volume-only model for (a) volume-plus-ground contributions for various horizontal baselines  $B$  in metres and (b) volume-plus-ground contribution for various surface-to-volume scattering ratios  $m$ .

## 3 Experimental Data

The test site lies near the Summit of the Austfonna ice cap on the island of Nordaustlandet in northeastern Svalbard, Norway ( $\sim 79\text{-}80^\circ\text{N}$ ,  $20\text{-}27^\circ\text{E}$ ) in the subpolar glacial regime. Validation is performed using a unique Pol-InSAR data set acquired over the Nordaustlandet ice sheet. The SAR data were collected using DLR's airborne E-SAR (Experimental SAR) system as part of the ICESAR campaign in March 2007. Repeat-pass fully-polarised multi-baseline data at L- (1.3 GHz) and P-band (0.35 GHz) frequencies were obtained.

## 4 Results and Discussion

The ground-to-volume scattering ratios estimated from polarimetric decompositions are used in combination with Pol-InSAR interferometric coherences and a uniform-volume-plus-ground model for determination of the ice extinction coefficients. Inverted extinction results at a nominal baseline of 5 m for L-band and 10 m for P-band using the Freeman-3 model for input  $m$  values are shown in **Figure 2**. A subset (50 azimuth pixels wide) is outlined in red, which is used in subsequent analysis to compare the various polarimetric decomposition methods over a smaller area, thereby reducing computation times as well. Note that the L- and P-band data are not perfectly coregistered, but represent approximately the same area.

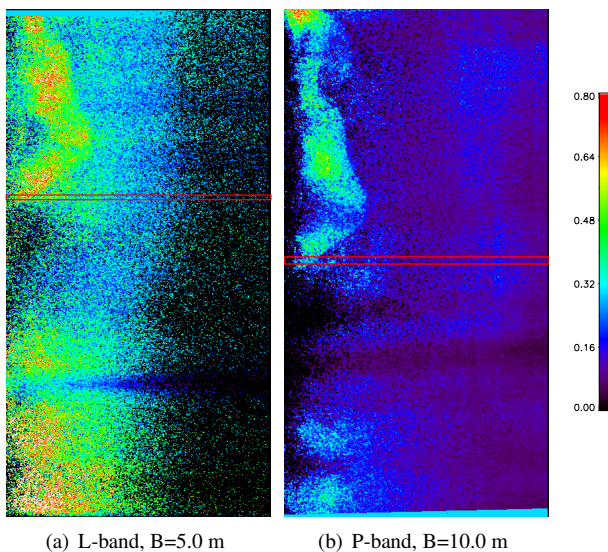


**Figure 2:** Inverted extinctions in dB/m at HH assuming a volume-plus-ground model with  $m$  values from Freeman-3. Flight (azimuth) direction is from bottom to top. Subsets used in **Figure 3** are highlighted in red.

Extinctions inverted using the subset of pixels are shown in **Figure 3**, again at a nominal baseline of 5 m for L-band and 10 m for P-band. Extinctions have been averaged through azimuth and smoothed through range to reduce noise, and are plotted versus incidence angle to reveal the existence of any trends. Examining the extinctions inverted assuming an infinite uniform volume (**Figure 3 (a) and (b)**), there is a clear trend of decreasing extinction with increasing incidence angle for the co-polar channels HH and VV. The incidence angle trend mimics those seen in the simulations of **Figure 1**, where the ground contribution was neglected during modelling, suggesting that the ground may also be contributing significantly to coherences in these experimental data. Modulated on top of this trend are additional features likely due to ice structure, particularly at P-band which penetrates deeper into the ice.

The resulting extinctions after removal of  $m$  using values estimated from Freeman-3 are shown in **Figure 3 (c) and**

**(d)**. At L-band the extinctions for all three linear polarisations are approximately equal and there is no distinguishable trend with range. At P-band the range trend has been removed using Freeman-3, although there exist differential extinctions between HH, VV and HV which may be due to oriented scatterers in the ice or due to inadequacies in the model such as over-compensated HH and VV or to unmodeled components at HV since the Freeman-3 model assumes  $m_{HV} = 0$ . Examining results over the entire image (**Figure 2**), the extinction results using Freeman-3 are generally satisfactory in that at P-band extinctions are very homogeneous through range, highlighting the presence of ice structures on the upper left-hand side. At L-band results are not as homogeneous, although there is improvement over the uniform volume assumption (see **Figure 3 (a), (c)**). At mid-range there is a decrease in the magnitude of the inverted extinctions which may partly be due to a ridge-type feature extending through azimuth (faintly visible in P-band) and/or to residual surface components at near-range in L-band.

Extinctions inverted using  $m$  from Freeman-2 are shown in **Figure 3 (e) and (f)** and from the eigenvector decomposition in **(g) and (h)**. The eigenvector and Freeman-2 decompositions at L-band suggest an over-estimation of the surface components in near-range since  $\kappa_{eHV}$  is greater than both co-pol extinctions and for the eigenvector decomposition there is now an inverse incidence angle trend (i.e. increasing extinctions with incidence angle).

At P-band Freeman-2 has decreased the magnitude of the co-pol extinctions in comparison with results assuming a uniform volume-only model, although a strong range trend still exists, suggesting that the model did not completely separate surface and volume components. The extinctions at P-band inverted using eigenvector decomposition are very low, indicating that perhaps the dominant surface scattering mechanism overwhelms the return signal, making it difficult to accurately estimate and thus separate out the volume component. The assumption from section 2.1 that the dominant scattering mechanism is surface scattering is supported by the presence of a  $T_1$  matrix which is nearly perfectly reflection-symmetric and which has low  $\alpha_1$  angles (indicative of surface scattering [3]) of  $\sim 37.2^\circ$  at L-band and  $17.1^\circ$  at P-band averaged over the entire scene.

### 4.1 Analysis and Limitations

Although extinctions have been successfully inverted, caution must be used in their interpretation due to the existence of several unresolved issues. Conventional surface scattering models such as the Small Perturbation Model [6] predict (to 1st order) an HV surface backscatter contribution of zero. In some instances, especially at P-band, the HV polarisation shows trends in  $\kappa_e$  through incidence angle, indicating that perhaps the assumption of  $m_{HV} = 0$  is not appropriate. This could be due to changes in ice structure through range, although because we see this trend when

looking from both north and south directions (from additional data not shown here), it could indicate the existence of increasingly complex scattering behaviour (e.g. multiple scattering, higher order surface scattering, or very rough interfaces).

Additionally, only results at relatively short baselines have been inverted here. As shown in section 2.2.1, extinctions inverted at larger baselines are more sensitive to any unmodeled ground contributions. In addition, larger baselines result in lower and thus noisier coherence magnitudes, contributing additional uncertainties to the extinction. Proof that these models can be extended over all baselines is still required.

Overall, extinctions inverted using ground-to-volume scattering ratios  $m$  derived from Freeman 3-component decomposition were the most consistent with cross-pol data and displayed the least amount of incidence-angle dependency. However, Freeman-3 assumes that the volume consists of randomly oriented dipoles; failures in this assumption will generate errors in the estimation of the ground-to-volume ratio  $m$ . Since a random volume should have identical extinctions for all polarisations, there are inconsistencies in our modelling, but it is an important first step in removing the ground contribution to derive unbiased land ice extinctions. Future work will focus on modelling oriented volumes to explain the observed differential extinctions between polarisations.

## 5 Summary

In this paper extinctions for land ice have been inverted after the removal of a surface scattering component from the interferometric coherence for the first time. Separation of the ground and volume contributions was obtained through decomposition of the polarimetric coherency matrix us-

ing both eigenvector and model-based Freeman-3 component and Freeman-2 component decompositions. Extinctions were inverted from experimental data over Nordaustlandet assuming both volume-only model and volume-plus-ground models with estimations of the ground-to-volume scattering ratio coming from polarimetry. The best results yielding inverted co-pol extinctions independent of incidence angle and close to extinction magnitudes at HV were obtained using ground-to-volume scattering ratios from Freeman-3.

Future work will concentrate on further modelling improvements including investigation into the possibilities of an oriented volume and the estimation of differential extinctions.

## References

- [1] E. W. Hoen and H. Zebker, "Penetration depths inferred from interferometric volume decorrelation observed over the greenland ice sheet," *IEEE Trans. Geosci. Remote Sens.*, vol. 38, no. 6, pp. 2572–2583, November 2000.
- [2] E. J. Rignot, K. Echelmeyer, and W. Krabill, "Penetration depth of interferometric synthetic-aperture radar signals in snow and ice," *Geophys. Res. Lett.*, vol. 28, no. 18, pp. 3501–3504, 2001.
- [3] S. R. Cloude and E. Pottier, "A review of target decomposition theorems in radar polarimetry," *IEEE Trans. Geosci. Remote Sens.*, vol. 34, no. 2, pp. 498–518, March 1996.
- [4] A. Freeman and S. L. Durden, "A three-component scattering model for polarimetric SAR data," *IEEE Trans. Geosci. Remote Sens.*, vol. 36, no. 3, pp. 963–973, May 1998.
- [5] A. Freeman, "Fitting a two-component scattering model to polarimetric SAR data from forests," *IEEE Trans. Geosci. Remote Sens.*, vol. 45, no. 8, pp. 2583–2592, August 2007.
- [6] F. Ulaby, R. Moore, and A. Fung, *Microwave Remote Sensing, Active and Passive, Volume II: Radar Remote Sensing and Surface Scattering and Emission Theory*. Norwood, MA: Addison-Wesley, 1982.
- [7] J. J. Sharma, I. Hajnsek, and K. P. Papathanassiou, "Multi-frequency Pol-InSAR signatures of a subpolar glacier," in *3rd Intl. Workshop on Sci. and Appl. of SAR Polarimetry and Polarimetric Interferometry (PolInSAR2007)*, Frascati, Italy, 22-26 January 2007.

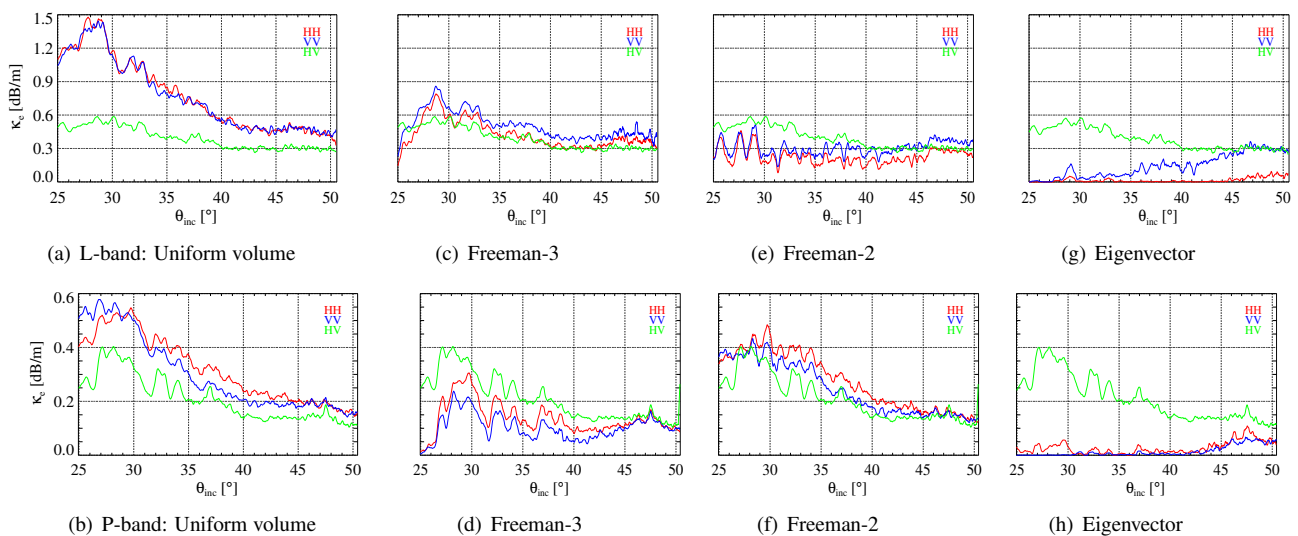


**Figure 3:** Inverted extinctions for L-band (top row) at a nominal 5 m baseline and P-band (bottom row) at a nominal 10 m baseline. Values have been averaged through azimuth for a volume-only and volume-plus-ground model with various ground-to-volume scattering ratios  $m$ .